SYNCHROTRON X-RAY DIFFRACTION STUDIES OF IN-SITU GROWN YBaCuO THIN FILMS ON (100) $SrTiO_3$

J.Q. Zheng, M.C. Shih, X.K. Wang, S. Williams,
S.J. Lee, Hiroshi Kajiyama*, Z. Zhao, K. Viani,
S. Jacobson, P. Dutta, J.B.Ketterson, and R.P.H. Chang
NSF Science and Technology Center for Superconductivity
and
Materials Research Center
Northwestern University
Evanston, IL 60208
and
T. Roberts, R. T. Kampwirth, and K.E. Gray
Materials Science Division, Argonne National Laboratory
Argonne, IL 60439

ABSTRACT

The effect of the deposition rate, substrate temperature and oxygen partial pressure on the growth of in-situ YBCO films on (100) $SrTiO_3$ during deposition has been studied by synchrotron X-ray diffraction (SXRD) in real time. The evolution of the film growth with thickness at various sputtering conditions was observed. The change of d-spacing and growth competition among c-axis, a-axis and other related orientations has also been observed in real time. The structural quality of in-situ sputtered YBCO films was characterized by the integrated diffraction intensity and the rocking curve. The nucleation and growth mechanisms of in-situ YBCO films are discussed.

INTRODUCTION

Most thin film synthesis techniques, such as laser ablation [1], magnetron sputtering [2] [3], ion beam sputtering [4], evaporation [5], molecular beam epitaxy [6] and MOCVD [7], have been successfully used to produce in-situ thin films of oxide superconductors with high T_c and J_c. Much current research now focuses on understanding the mechanisms of thin film growth during deposition and on controlling the quality of the deposited film. Such information is valuable in device fabrication.

---

* On leave from Advanced Research Laboratory, Hitachi Ltd., Japan

It is well known that the structural and superconducting properties of high T_c thin films are strongly influenced by the stoichiometry, substrate material and orientation, and the preparation process. YBCO films have been produced with c-axis, a-axis, (110), and mixed (110)/(103) orientations, depending on the substrate temperature [8], and have been examined by ion channelling [9]. Fujita et al have reported that epitaxial orientations can be varied by controlling both the substrate temperature, T_s, and the oxygen partial pressure $P(O_2)$. At higher T_s and lower $P(O_2)$, the YBCO films favored c-axis growth; by lowering T_s and increasing $P(O_2)$, mixed a/c- and a-axis oriented films were easily obtained [4]. The early stages of growth and the microstructure of epitaxial YBCO films with different orientations on various single crystal substrates have been observed by using high resolution electron microscopy [10] [11] [12] [13]. The growth behavior has been explained by the growth rate dependence, by stacking faults and by the relationship of the lattice constants between YBCO and the substrate (due to the oxygen deficiency and different thermal expansions) [4] [10] [13] [14]. A Bellcore group recently reported, using cross section techniques, that both a-axis and c-axis nuclei appear and that the a-axis grows epitaxially on a c-axis base at lower deposition temperatures [14]. Terashima et al have studied the in-situ growth of YBCO films by reflection high energy electron diffraction (RHEED). They pointed out that elastic strain accommodates the lattice mismatch between the film and the substrate [15].

Clearly, it is desirable to be able to control the initial nucleation and epitaxy, crystal orientation, defect density and phase purity of these films. In addition, it is important to understand the relationship between various crystal properties and synthesis parameters such as substrate surface preparation, substrate temperature, sputtering rate, ambient gas pressure and composition. These studies require the observation of crystal growth in real time. Synchrotron X-ray diffraction (SXRD) is one of most powerful tools for studying the structures of high T_c oxide thin films. Synchrotron sources have very high intensity, at least three to four orders of magnitude higher than that of a standard diffractometer. The X-ray beam can also be highly monochromatic and well collimated, providing a very high angular resolution (better than 0.01°).

EXPERIMENTAL

Since most sputtering chambers are not compatible with conventional X-ray diffractometers and synchrotron sources, we have fabricated a dedicated, miniature, sputtering chamber with two sector windows permitting standard θ-2θ scans as well as in-plane XRD studies [16]. Epitaxial, highly-oriented YBCO films on (100) $SrTiO_3$ have been prepared in situ using this system. The system has the following unique features: a) to avoid negative ion resputtering of the film surface during deposition, the substrate is located at right angles to the sputtering targets and at the edge of the glow discharge; b) to produce a higher

deposition rate, a pair of magnet-backed targets are placed facing each other such that the magnetic field lines are additive, the field serving to confine the charged species in the plasma; and c) the sputtering system is designed with a special geometry and a very small size (the total volume is only about 1 liter) so as to fit in a standard Huber (six-circle) goniometer at a synchrotron X-ray beam line.

All experiments were carried out at beam line X18A of the National Synchrotron Light Source (NSLS) facility of the Brookhaven National Laboratory. The X-ray beam was monochromated to a wavelength of 1.556 Å and focused to a spot approximately 1 mm x 2 mm. A scintillation detector was used for the diffraction scans. The high intensities available at a synchrotron make it possible to observe the initial growth stages of the film where rather broad and weak diffraction peaks are encountered; for thicker films, the high resolution permits separating the substrate peaks from the epitaxial film peaks. During deposition, the X-ray diffractometer was programmed to scan angular ranges corresponding to diffraction peaks of interest, such as (300), (007), (220), and others in the range of 45 to 80 degrees. The intensities of the various growing peaks versus film thickness were recorded along with the duration of deposition. D.C. sputtering of $YBa_2Cu_3O_x$ targets was performed at a total pressure of 90 mTorr with various ratios of the Ar/O_2 mixture. The substrate could be heated up to 800 °C. The substrate temperature was measured by a digital pyrometer; it was 80 - 90 °C lower than that indicated by a K-type thermocouple located inside the sample holder which was the sensor for the temperature controller which drove two cartridge heaters. The deposition rate, which was determined by the applied sputtering power, was in the range of 1 Å/sec to 6 Å/sec. In-situ YBCO films deposited on $SrTiO_3$ had a black, smooth and shiny surface. From AES and EDAX analyses, the sputtered YBCO films had the same stoichiometry as the targets [16].

RESULTS AND DISCUSSION

In order to address the evolution of the film growth in real time, we have systematically investigated the effect of the deposition rate (R), substrate temperature (Ts) and oxygen partial pressure (P(O2)) on the nucleation and growth of in-situ YBCO films grown on (100) $SrTiO_3$. From the experimental results, we found that all these parameters are significant factors in determining whether YBCO films grow along the a-axis, c-axis, as an a/c-mixture, or along multiple axes.

Deposition Rate Dependence: During sputtering the total working pressure was kept at 90 mTorr with an Ar/O_2 ratio of 2 : 1. The substrate temperature was constant at 730 °C. In-situ YBCO films were prepared at deposition rates of 1 Å/sec, 2 Å/sec, 4 Å/sec and 6 Å/sec respectively. The final film thickness for all runs was about 7200 Å. Our experimental results showed that the orientation was closely related to the deposition rate.

At a low deposition rate (1 Å/sec), the growth occurred primarily along the a-axis. Figs. 1 (a) and (b) show how the a-axis and c-axis intensities grow with film thickness during sputtering. From Fig. 1(c) it is clear that the c-axis nucleates first and grows faster at the early stages. When the thickness of the growing film reaches a critical value (~1500 Å), the intensity of the c-axis (007) peak reaches a maximum and then falls slightly (due to the attenuation of the growing a-axis oriented layers which covered the c-axis base). For the a-axis growth, the (200) peak grows slowly at thicknesses less than 1500 Å. After that, the (200) peak increases linearly with time (thickness). Finally, the a-axis orientation is dominant

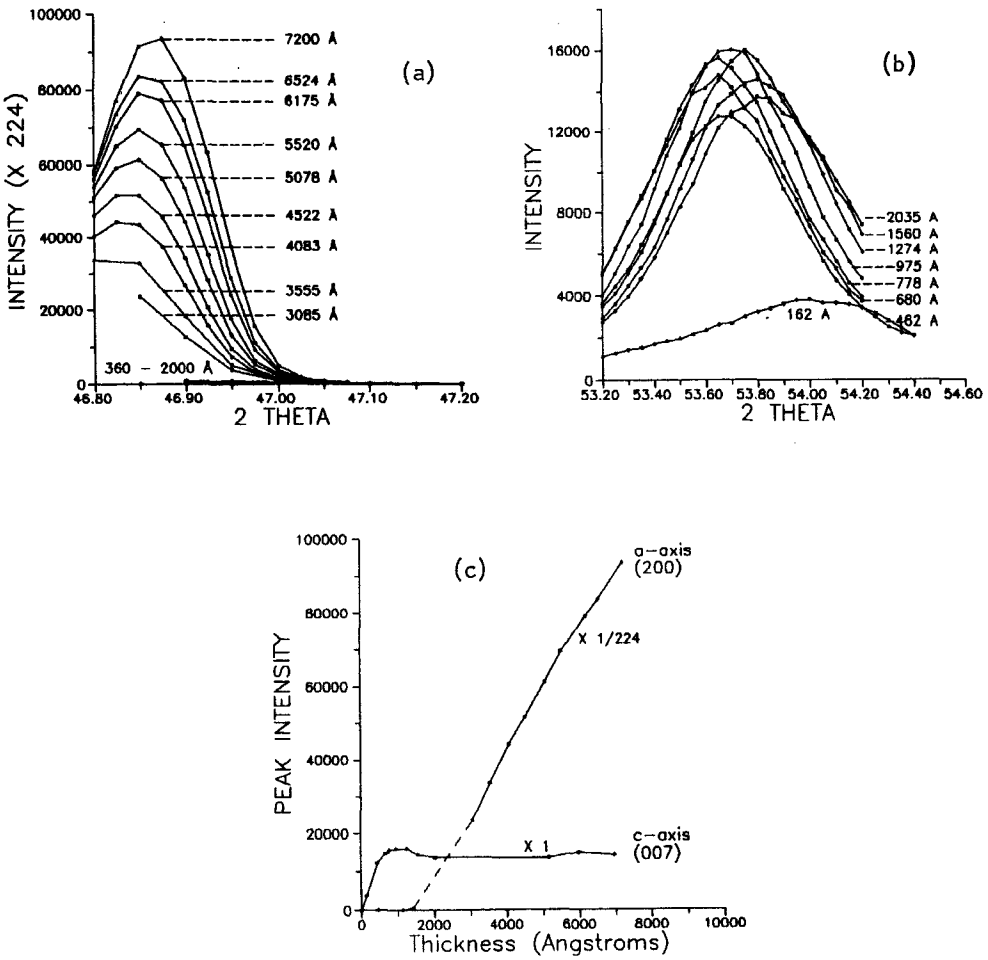

Fig. 1 Growth of Y-Ba-Cu-O peaks with thickness during sputtering (T_s = 730 °C, R = 1Å/sec); (a) (200) peak and (b) (007) peak. (c) The intensity of the (200) and (007) peaks as a function of thickness.

relative to the c-axis growth. The full width at half maximum (FWHM) of the rocking curve of the a-axis oriented film grown at a rate of 1 Å/sec is 0.4° . The integrated intensity of the (200) peak is four orders of magnitude higher than that of the (007) peak. During the growth process, we observed that the d-spacing of the c-axis and a-axis orientations changed with film thickness and tended to a stable value (that of bulk YBCO material). The expanded d-spacings, for both the c-axis and a-axis are, attributed to the lattice mismatch between the YBCO film and substrate. The strains are gradually relieved as the thickness increases.

At higher deposition rates (2 and 4 Å/sec), the time evolutions were very similar to those at lower rates. However, the a-axis growth was suppressed in favor of c-axis growth. The films showed a mixture of a-axis and c-axis orientations. The diffraction intensity of the c-axis peaks increased with increasing deposition rate. On further increasing the rate to 6 Å/sec, the a-axis peaks were no longer visible. This implies that only the c-axis grains nucleated and grew. The rocking curve of the c-axis oriented film is 0.9°. These c-axis-dominated films were always accompanied with a (220) peak as the films became thicker.

For fixed values of other sputtering parameters, the deposition rate is proportional to the applied sputtering power, which also affects the energy of sputtered atoms (molecules). The kinetic energy of the deposited species presumably influences the nucleation and the film growth. Our results reveal that a low power promotes epitaxial growth along the a-axis. For molecules sputtered at higher power, the film growth favors a c-axis orientation. As the film thickens, it is apparently easier for other orientations to nucleate. Then, it is possible that the surface temperature of the growing YBCO film may be higher, leading to a higher surface mobility of the depositing material.

Substrate Temperature Dependence: In order to explore the effect of substrate temperature on the film growth, we deposited YBCO films at 4 Å/sec while varying the substrate temperature in the range of 625 - 800 °C. The thickness of the sputtered films for all runs was about 7000 Å. The total working pressure was kept constant at 90 mTorr with an Ar/O_2 ratio of 2 : 1.

For substrate temperatures below 665 °C, we observed only amorphous film growth. At T_s = 665 °C, the time evolution of the diffraction patterns showed the presence of oscillation peaks at the early stages (t<100 Å), as shown in Fig.2. The series of oscillations (or multiple peaks) occurs around the position of the (300) peak of the "123" phase (in place of the usual single peak). The change in the average d-spacing corresponding separation of the oscillations is 2×10^{-3} Å. We can not rule out the possibility that the peaks might arise from an ensemble of islands with different (but quasi-discrete) lattice spacings. Alternatively, it may be interpreted as the diffraction lobes associated with a (globally rather uniform) ultra thin

crystalline film (which then gives way to amorphous growth). With further deposition, the amplitude of the oscillations diminishes. After 800 Å, the oscillations smear out. We could not find any crystalline peak related to the "123" phase; the deposited film was amorphous (note that the background comes from the (300) peak of $SrTiO_3$).

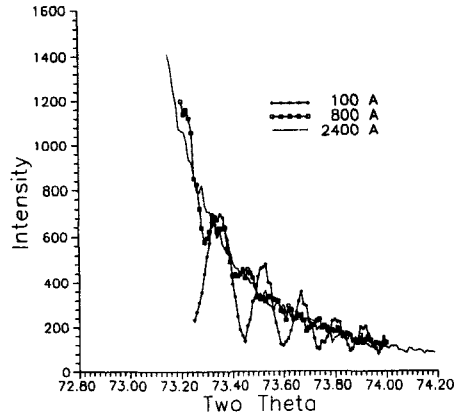

Fig. 2 Oscillation around (300) peak at the early stages of growth (T_s = 665 °C). The multiple peaks disappeared with increasing thickness.

Raising the substrate temperature to 685 °C, we observed the disappearance of the "multiple" peaks and the diffraction pattern showed two peaks at earlier stages (t = 120 Å), in the vicinity of the (300) peak of the bulk "123" phase. As the film thickened, we observed a rapid increase in the intensity of the high angle peak (which is closer to the (300) peak) and the disappearance of the low angle peak. Finally, a strong a-axis oriented YBCO film was formed. At 695 °C, the growth processes were very similar. However, at the earlier stages (t = 240 Å) the high angle peak was stronger than the low angle (see Fig. 3 (a)). The (300) peak then develops at the higher angle and, becomes both strong and sharp, as shown in Fig. 3(b). This film showed the sharpest rocking curve with a FWHM of only 0.08 degree, indicating near perfect crystallinity. This implies either that finite size effects are reduced, or that the structural quality of the a-axis oriented film evolves to a more nearly perfect form as the film thickens. Here we should point out that under these conditions, an (007) peak was also observed at the initial growth stages, although it was very broad and weak. At first, C-axis grains nucleated and grew on the substrate surface; but at about 100 to 300 Å, the c-axis oriented grains ceased to grow.

At 730 °C, the film growth was based on both c-axis and a-axis nuclei, without "multiple" peaks. The YBCO film showed a mixed c-/a-axis orientation, but it was dominated by the a-axis orientation. It is clear that the competition between c-axis and a-axis growth on (100) $SrTiO_3$ depends on the substrate

temperature as well as the deposition rate and oxygen partial pressure. At higher T_s, both the c-axis and a-axis nucleated; the c-axis grew first and the a-axis developed later; also the intensity of the c-axis peaks became much stronger with increasing substrate temperature.

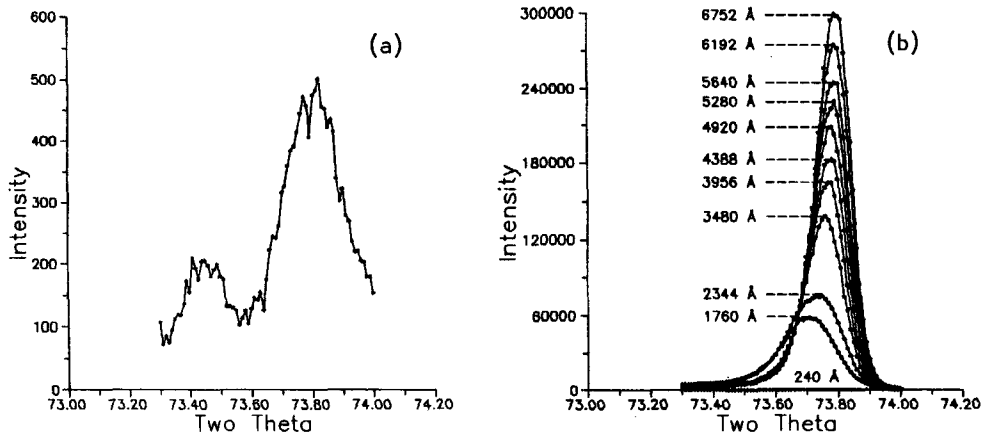

Fig. 3 (300) peak growth during sputtering (T_s = 695 °C, R = 4Å/sec); (a) an early stage with two peaks (t = 240Å) and (b) (300) growth with thickness.

At 800 °C, there is only one peak, corresponding to the (007) peak of the c-axis, which appeared at the initial growth stages. Fig. 4 shows the time evolution of the diffraction profiles associated with the (007) peak of the "123" phase. With increasing thickness, the (007) peak intensities approach saturation and other peaks appeared. The (300) peak was found at about 4000 Å and then continued to grow with increasing thickness. This provides further evidence that the a-axis grains nucleate on a c-axis base. The results show that the same nucleation and growth behavior is obtained (for in-situ YBCO films on (100) $SrTiO_3$) by changing either the deposition rate or the substrate temperature.

Oxygen Partial Pressure: The total working pressure was kept at 90 mTorr during sputtering. The ratio of the Ar/O_2 mixture ranged from 10:1 to 1:3 and was adjusted by two individual needle valves. The substrate temperature was constant at 730 °C. The sputtering power for all runs was fixed at 20 W. One might expect higher oxygen partial pressures to drastically reduce the sputtering yields and cause resputtering, thus changing the composition of the growing film (due to the negative ion effect) [17]. With our magnetron gun design, however, the rates only changed by 36% (from 2.2 Å/sec down to 1.4 Å/sec).

When the ratio of Ar/O_2 lies in the range 5:1 to 1:3, YBCO films grew with a mixture of a-axis and c-axis orientations, but all samples were dominated by the a-axis orientation. At higher $P(O_2)$, the films showed a preferential orientation with the

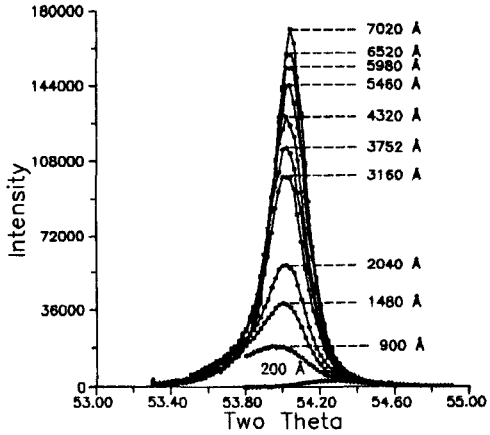

Fig. 4 (007) peaks growth during sputtering (T_s = 800 °C, R = 4Å/sec).

a-axis normal to the surface and the integrated intensities were much higher (> 1000 times) than those for the c-axis peaks. Fig.5(a) shows the evolution of the (300) peak growth of a YBCO film from the early stages through a thickness of around 5500Å for an Ar/O_2 ratio of 2:1. The behavior is consistent with our experiments on the deposition rate dependence. We found that the d-spacing of the a-axis orientation was expanded at the early stages and gradually shifted to a stable value when the film grew thicker. This a-axis oriented film showed a very sharp rocking curve with a full width at half maximum of less than 0.1 degree, as shown in Fig.5(b). When the evolving film reached a certain thickness, the peak intensities of the diffraction pattern for the c-axis orientation saturated and then decreased slightly. In the mean time, the intensity of the a-axis peaks increased linearly with increasing film thickness (see Fig.5(c)). It is clear that c-axis nuclei form directly on the substrate surface; the a-axis orientation nucleates and develops later. The volume fraction of c-axis and a-axis nuclei at the initial stages was controlled by the oxygen partial pressure as well as the substrate temperature and deposition rate.

We will refer to the thickness where the YBCO film significantly changes from c-axis to a-axis growth as the "critical thickness" (t_c). The same phenomenon was observed in our studies of the deposition rate and substrate temperature dependence as mentioned above. In the present study the values of the critical thickness depended on the oxygen partial pressure of the Ar/O_2 mixture (see Fig.6). It is noted that the higher $P(O_2)$, the smaller the critical thickness and the earlier a maximum is reached for c-axis intensity. For an Ar/O_2 ratio ranging from 1:2 to 5:1, the critical thickness is between a few hundred and less than two thousand angstroms. From the X-ray profiles, it is clear that the oxygen atmosphere in the

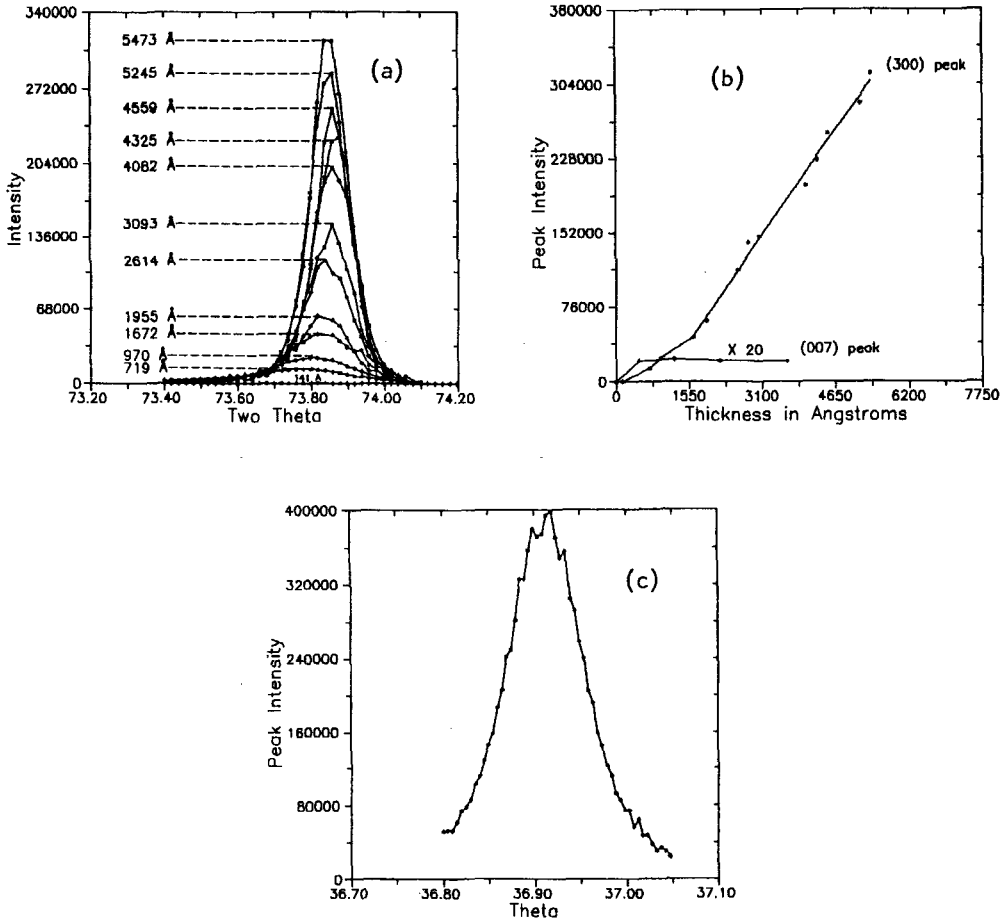

Fig. 5 (a). Evolution of the (300) peak of $YBa_2Cu_3O_x$ with thickness during deposition (Ar/O_2 = 2:1, P = 90 mTorr, T_s = 730 °C, R = 2 Å/sec); (b) rocking curve of the (300) peak; (c) the intensity of the (300) and the (007) peak as a function of thickness.

sputtering process is not only necessary for keeping the YBCO sputtering targets in a conductive condition, but is also helpful for growing epitaxial a-axis YBCO films and suppressing c-axis growth. When the oxygen pressure decreased to an Ar/O_2 ratio of 5:1, the intensity of the (007) peak apparently increased. However, the film was still dominated by the a-axis orientation and no other peaks (such as (220)) were detected. Our results are consistent with the nucleation model for depositing YBCO on (100) $SrTiO_3$ substrates suggested by Ramesh et al [18]. Either the SrO or TiO_2 layers easily accommodate the CuO_2 or BaO layers at the earlier stages. From this point of view, the YBCO film favors the nucleation of c-axis grains. According to the bulk crystallization behavior of YBCO, flat-

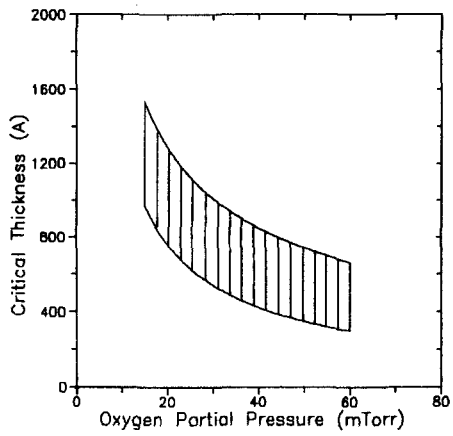

Fig. 6 The critical thickness (defined as a change from c-axis to a-axis growth) as a function of oxygen partial pressure for a total pressure of 90 mTorr (T_s = 730 °C, R = 2Å/sec).

shaped (00ℓ) grains are favored. In fact, the deposition conditions (R, T_s, $P(O_2)$, etc.) may be changed to precisely control the orientations in the growth process. Higher oxygen pressures, $P(O_2)$, as well as lower R and T_s favor an earlier cross over from c-axis to a-axis growth. A possible explanation is that higher $P(O_2)$, and lower R and T_s, reduce the surface mobility [19]. This would enhance the crystal growth rate (in terms of the height to width ratio of the grains) normal to the (00ℓ) plane (a-axis orientation) rather than parallel to the (00ℓ) plane (c-axis orientation), and therefore modify the growth.

At very low oxygen partial pressures, the growth processes were rather similar, but the films changed their nucleation and growth behavior. For an Ar/O_2 ratio of 10:1, the diffraction patterns showed only a peak at 2θ = 64.9°, which corresponds to the (500) peak of the "green" phase Y_2BaCuO_5 (which is orthorhombic with a = 7.132 Å, b = 12.181 Å, and c = 5.658 Å); apparently a-axis Y_2BaCO_5 nucleates first on the $SrTiO_3$ substrate. It is easy to understand that, under the combined conditions of higher T_s and lower $P(O_2)$, the $YBa_2Cu_3O_x$ material decomposes into Y_2BaCuO_5, $BaCuO_2$, and CuO, and only the perovskite structure Y_2BaCuO_5 will deposit and grow on (100) $SrTiO_3$ at 730 °C. On increasing the Ar/O_2 ratio to 7:1, a small amount of c-axis "123" phase exists along with the "green" phase in the initial stages of growth. From the evolution of the (500) peak of Y_2BaCuO_5 with thickness, the (500) peak grew and reached a maximum (~800 Å) as the film thickened. Later on, the (500) peak intensity rapidly decreased to an asymptotic value, as shown in Fig.7(a). In the mean time, the (220) peak of "123" phase grew rapidly. However, no a-axis peaks from "123" could be observed. The competition of different phases at very low oxygen partial pressure is shown in Fig.7(b). Our results reveal that the oxygen partial pressure is

a very important factor for the in-situ processing of YBCO films without post-annealing. The oxygen partial pressure must be higher than a certain value, for a given substrate temperature, to create "123" nuclei on $SrTiO_3$ substrates.

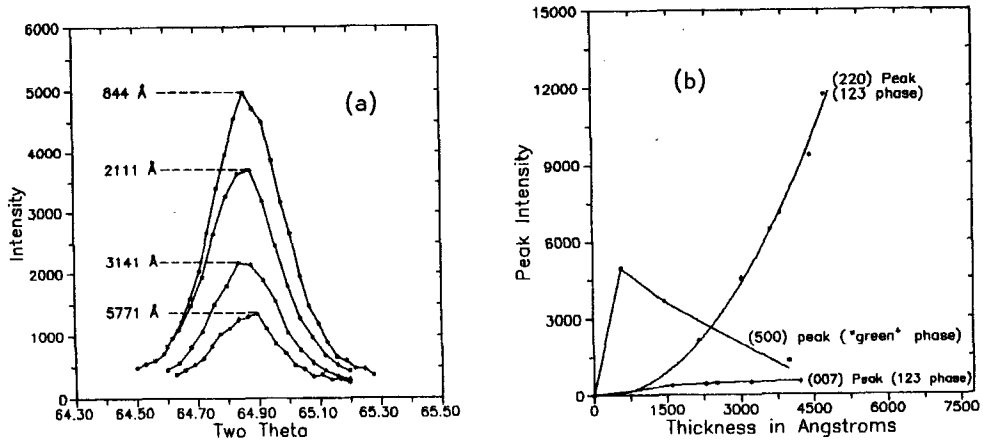

Fig. 7 (a). Evolution of the (500) peak of Y_2BaCuO_5 with thickness during deposition (Ar/O_2 = 7:1, P = 90 mTorr, T_s = 730 °C, R = 2Å/sec); (b) the intensity of the (007) and the (220) peak ("123" phase), and the (500) peak ("green" phase) as a function of thickness.

CONCLUSION

We have studied in-situ synchrotron X-ray diffraction of sputtered YBCO thin films on (100) $SrTiO_3$ under various growth conditions. At low deposition rates and low substrate temperatures, the a-axis grows preferentially. At the early states, the c-axis nuclei grew to a certain thickness and then the a-axis growth take over. These a-axis epitaxial films have the highest crystal quality (with a rocking curve < 0.1°). At high deposition rates and high substrate temperatures, the a-axis growth was suppressed and the c-axis growth became dominant. The c-axis oriented films were always accompanied with a (220) peak.

Higher oxygen partial pressures in the Ar/O_2 mixture during sputtering promotes the growth with the a-axis orientation, in spite of c-axis nuclei which develop at the earlier stages. There exists a "critical thickness" in the process of the film formation, after which there is a change from c-axis to a-axis growth. The same phenomenon was observed in the deposition rate and substrate temperature dependence. At lower oxygen partial pressures, the initial growth occurred along the a-axis of the Y_2BaCuO_5 "green" phase with a small amount of c-axis "123" phase; later the (220) plane of the "123" phase appeared.

In summary, we have observed:

1. the evolution of the in-situ growth of YBCO films on $SrTiO_3$;
2. the nucleations and growth competition of the c- and a-axis orientations at early stages;
3. a-axis growth on c-axis grains (with the existence of a critical thickness);
4. the changes of d-spacing along the c- and a-axis orientations during film formation (due to lattice mismatch);
5. the dependence of the orientation and structural quality of sputtered YBCO films on preparation conditions such R, T_s and $P(O_2)$, etc.

The results suggest mechanisms for the nucleation and growth of YBCO films on $SrTiO_3$ and allows the optimization of the preparation parameters for fabricating high quality YBCO film with desired orientations.

Acknowledgement: We gratefully acknowledge Dr. S. Erlich, Xiao-Chun Yang and the staff of the National Synchrotron Light Source at the Brookhaven National Laboratory for their assistance and facility support. This work was supported by the NSF Science and Technology Center for Superconductivity under grant DMR 88-09854; the Northwestern University Materials Research Center grant number DMR 88-21571; and the Illinois Technology Challenge Fund.

REFERENCES

1. D. Dijkkamp, T. Venkatesan, X.D. Wu, S.A. Shaheen, N. Jisrawi, Y.H. Min-Lee, W.L. McLean, and M.Croft, Appl. Phys. Lett., **51**, 619 (1987).

2. H.C. Li, G. Linker, F. Ratzel, R. Smithey, and J.Geerk, Appl. Phys. Lett., **52**, 1098 (1988).

3. C.B. Eom, J.Z. Sun, K.Y. Yamamoto, A.F. Marshall, K.E. Luther, T.H. Geball, and S.S. Laderman, Appl. Phys. Lett., **55**, 595 (1989).

4. J. Fujita, T. Yoshitake, A. Kamijo, T. Satoh, and H. Igarashi, J. Appl. Phys., **64**, 1292 (1988).

5. N. Missert, R. Hammond, J.E. Mooij, V. Maijasevic, P. Rosenthal, T.H. Geball, A. Kapitulnic, M.R. Beasley, S.S. Laderman, C. Lu, E. Garin, and R. Barton, IEEE Trans. Magn., **MAG-25**, 2418 (1989).

6. J. Kwo, M. Hong, D.J. Trevor, R.M. Fleming, A.E. White, J.P. Mannaerts, R.C. Farrow, A.R. Kortan, and K.T. Short, Physica C, **162-164**, 623 (1989).

7. C.S. Chern, J. Zhao, Y.Q. Li, P. Norris, B. Kear, and B. Gallois, Appl. Phys. Lett., **57**, 721 (1990).

8. G. Linker, X.X. Xi, O. Meyer, Q. Li, and J. Geerk, J. Less-Common. Metals, **151**, 357 (1989).

9. Q. Li, F. Weschenfelder, O. Meyer, X.X. Xi, G. Linker, and J. Geerk, J. Less-Comm. Metals, **151**, 295 (1989).

10. B.M. Clemens, C.W. Nieh, J.A. Kittl, W.L. Johnson, J.Y. Josefowicz, and A.T. Hunter, Appl. Phys. Lett., **53**, 1871 (1988).

11. D.M. Hwang, T. Venkatesan, C.C. Chang, L. Nazar, X.D. Wu, A. Inam, and M.S. Hegde, Appl. Phys. Lett., **54**, 1702 (1989).

12. M. Grant Norton, Lisa A. Tietz, Scott R. Summerfelt, and C. Barry Carter, Appl. Phys. Lett., **55**, 2348 (1989).

13. C.W. Nieh, L. Anthony, J.Y. Josefowicz, and F.G. Krajenbrink, Appl. Phys. Lett., **56**, 2138 (1990).

14. C.C. Chang, X.D. Wu, R. Ramesh, X.X. Xi, T.S. Ravi, T. Venkatesan, D.M. Hwang, R.E. Muenchausen, S. Foltyn, and N.S. Nogar, Appl. Phys. Lett., **57**, 1814 (1990).

15. Takahito Terashima, Kenji Iijima, Kazunuki Yamamoto, Kazuto Hirata, Yoshichika Bando, and Toshio Takada, Jpn. J. Appl. phys., **28**, 1987 (1989).

16. J.Q. Zheng, M.C. Shih, X.K. Wang, S. Williams, P. Dutta, R.P.H. Chang, and J.B. Ketterson, J. Vac. Sci.& Technol. A, **9**, 128, Jan/Feb (1991).

17. S.M. Rossnagel and J.J. Cuomo, AIP Conference Proceedings No. **165**, PP.106, (1987).

18. R. Ramesh, C.C. Chang, T.S. Ravi, D.M. Hwang, A. Inam, X.X. Xi, Q. Li, X.D. Wu, and T. Venkatesan, Appl. Phys. Lett. **57**, 1064 (1990).

19. R.H. Hammond and R.Bormann, Physica C, **162-164**, 703 (1989).